Quantifying TOLNet Ozone Lidar Accuracy during the 2014 DISCOVER-AQ and FRAPPÉ Campaigns

Lihua Wang[1], Michael J. Newchurch[1], Raul J. Alvarez II[2], Timothy A. Berkoff[3], Steven S. Brown[2], William Carrion[3,4], Russell J. De Young[3], Bryan J. Johnson[2], Rene Ganoe[4], Guillaume Gronoff[3,4], Guillaume Kirgis[2,5], Shi Kuang[1], Andrew O. Langford[2], Thierry Leblanc[6], Erin E. McDuffie[2,5,7], Thomas J. McGee[8], Denis Pliutau[4], Christoph J. Senff[2,5], John T. Sullivan[8,9], Grant Sumnicht[4], Laurence W. Twigg[4], Andrew J. Weinheimer[10]~~[9]~~

[1]University of Alabama in Huntsville, Huntsville, Alabama, USA

[2]NOAA Earth System Research Laboratory, Boulder, Colorado, USA

[3]NASA Langley Research Center, Hampton, Virginia, USA

[4]Science Systems and Applications Inc., Lanham, Maryland, USA

[5]Cooperative Institute for Research in Environmental Sciences, University of Colorado, Boulder, Colorado, USA

[6]Jet Propulsion Laboratory, California Institute of Technology, Wrightwood, California, USA

[7]Department of Chemistry, University of Colorado, Boulder, Colorado, USA

[8]NASA Goddard Space Flight Center, Greenbelt, Maryland, USA

[9]Joint Center for Earth Systems Technology, Baltimore, Maryland, USA

~~[9]~~[10]National Center for Atmospheric Research, Boulder, USA

Correspondence to Shi Kuang (kuang@nsstc.uah.edu)

Formatted: Superscript

Abstract

The Tropospheric Ozone Lidar Network (TOLNet) is a unique network of lidar systems that measure high-resolution atmospheric profiles of ozone. The accurate characterization of these lidars is necessary to determine the uniformity of ~~cross-instrument~~the network calibration. From July to August 2014, three lidars, the TROPospheric OZone (TROPOZ) lidar, the Tunable Optical Profiler for Aerosol and oZone (TOPAZ) lidar, and the Langley Mobile Ozone Lidar (LMOL), of TOLNet participated in the "Deriving Information on Surface conditions from Column and Vertically Resolved Observations Relevant to Air Quality" (DISCOVER-AQ) mission and the "Front Range Air Pollution and Photochemistry Éxperiment" (FRAPPÉ) to measure ozone variations from the boundary layer to the top of the troposphere. This study presents the analysis of the intercomparison between the TROPOZ, TOPAZ, and LMOL lidars, along with comparisons between the lidars and other *in situ* ozone instruments including ozonesondes and a P-3B airborne chemiluminescence sensor. ~~In terms of the range-resolving capability, t~~The TOLNet lidars measured vertical ozone structures with an accuracy generally better than ±15% within the troposphere. Larger differences occur at some individual altitudes in both the near-field and far-field range of the lidar systems, largely as expected. In terms of column average, the TOLNet lidars measured ozone with an accuracy better than ±5% for both the intercomparison between the lidars and between the lidars and other instruments. These results indicate ~~very good measurement accuracy~~that ~~for~~ these three TOLNet lidars~~,~~ ~~making them~~are suitable for use in air quality, satellite validation, and ozone modeling efforts.

1. Introduction

1.1 TOLNet

The Tropospheric Ozone Lidar Network (TOLNet) provides time-height measurements of ozone from the planetary boundary layer (PBL) to the top of the troposphere at multiple locations for satellite validation, model evaluation, and scientific research (Newchurch et al., 2016; http://www-air.larc.nasa.gov/missions/TOLNet/). Particularly, these ~~high-fidelity~~ ozone measurements can serve to validate NASA's first Earth Venture Instrument mission, Tropospheric Emissions: Monitoring Pollution (TEMPO), planned to launch in 2019. A second objective of TOLNet is to identify a brassboard ozone lidar instrument that would be suitable to populate a network to address an increasing ~~desire~~ need for ozone profiles by ~~air quality~~ scientists and managers within the air quality, modeling, and satellite communities (Bowman, 2013).

TOLNet consists of five ozone lidars across the United States and one in Canada: the Table Mountain tropospheric ozone differential absorption lidar (DIAL) at NASA's Jet Propulsion Laboratory, the Tunable Optical Profiler for Aerosol and oZone (TOPAZ) lidar at NOAA's Earth System Research Laboratory (ESRL), the Rocket-city Ozone (O_3) Quality Evaluation in the Troposphere (RO_3QET) lidar at the University of Alabama in Huntsville (UAH), the TROPospheric OZone (TROPOZ) DIAL at NASA's Goddard Space Flight Space Center (GSFC), the Langley Mobile Ozone Lidar (LMOL) at NASA's Langley Research Center (LaRC), and the Autonomous Mobile Ozone Lidar Instrument for Tropospheric Experiments (AMOLITE) at Environment and Climate Change Canada.

All TOLNet lidars have unique configurations ~~that are associated with their~~of original measurement design purposes, including their transmitter, receiver, and signal processing systems. Most components of these lidars are customized and differ significantly in pulse energy, repetition rate, receiver size, solar (or narrow-band) interference filter, and range resolution. These differences result in varying signal-to-noise ratios (SNRs), which impact the useful operating ranges and statistical uncertainties in ozone retrieval. The selection of the DIAL wavelengths determines the sensitivity to interference by other species, primarily aerosols. In addition, multiple lidar data processing and retrieval algorithms could also lead to different effective resolutions and lidar retrieval uncertainties (Godin et al., 1999; Leblanc et al., 2016a,b). Therefore, it is important to quantify the measurement differences between the TOLNet lidars and understand their sources before we can form a consistent TOLNet dataset. A previous intercomparison between TROPOZ and LMOL reported by Sullivan et al. (2015) concluded that the observed ozone column averages from the two lidars were within ±8% of each other, and their ozone profiles were mostly within ±10% of each other. ~~That particular study served as the first reported measurement intercomparison of two ground-based tropospheric ozone lidar systems within the United States.~~

1.2 DISCOVER-AQ 2014 and FRAPPÉ Campaigns

The scientific goal of the TOLNet lidars in this study was to provide continuous, high-resolution tropospheric ozone profiles to support the NASA-sponsored DISCOVER-AQ mission (https://www.nasa.gov/larc/2014-discoveraq-campaign/), and the National Science Foundation (NSF) and state of Colorado (CO) jointly sponsored FRAPPÉ (Dingle et al., 2016) from July to August 2014. By collaborating with FRAPPÉ, the 2014 CO study was the final stop in a series of four field campaigns by DISCOVER-AQ to understand sources, transport and chemical transformations of air pollutants, particularly those that lead to ground-level ozone formation (Crawford and Pickering, 2014).

Prior to the two campaigns, TOPAZ, TROPOZ, and LMOL were all deployed to the same location in Erie, CO to obtain intercomparison data at the Boulder Atmospheric Observatory (BAO) (40.050^{o}N, 105.003^{o}W, 1584 m above sea level, ASL). Subsequent to the BAO intercomparison, TROPOZ and LMOL re-deployed to locations near Fort Collins, CO (~60 km north-northwest of BAO) and Golden, CO (~40 km southwest of BAO), respectively, for their different scientific missions. During the DISCOVER-AQ and FRAPPÉ campaigns, balloon-borne ozonesondes were launched at selected~~ive~~ sites. In addition, the NASA P-3B aircraft performed multiple spiral ascents and descents over several ground sites and provided ~~numerous vertical profiles of ozone~~ measurements of ozone profiles. In this study, we compare retrievals between the three lidars and evaluate the ozone lidar accuracy using ozonesonde and P-3B aircraft measurements. These two campaigns offered a unique opportunity for the lidar validation work, as they involved so many different instruments.

2. Instruments

2.1 TOLNet Lidars

Table 1 lists the main hardware specifications of the three TOLNet lidars and their ozone retrieval processes, which could potentially impact the intercomparison result.

Formatted: Font: Not Bold

2.1.1 TROPOZ/NASA GSFC

The transmitter for TROPOZ consists of two 50-Hz Nd:YAG- lasers used to pump two Raman cells filled with Deuterium (D_2) and Hydrogen (H_2) gases, respectively, to generate two outgoing ~~lasers~~ pulses at 289 and 299 ~~-~~nm. The typical pulse energies are 12 mJ at 299 nm (off-line) and 16 mJ at 289 nm (on-line) (Sullivan et al., 2014). The receiving system consists of a 45-cm-diameter Newtonian telescope for measuring far field and four smaller 2.5-cm refracting telescopes to measure near field. The 45-cm telescope has a 1-mrad field of view (FOV), and the 2.5-cm telescopes have a much wider FOV at 10 mrad. In each channel, solar interference filters with a 1-nm bandwidth decrease the amount of ambient solar light, which improves the SNR. The fundamental range resolution for the data acquisition system is 15 m (100 ns). TROPOZ measures ozone up to 16 km during daytime hours and higher altitudes at night.

2.1.2 TOPAZ/NOAA ESRL

The TOPAZ lidar is a truck-mounted ~~zenith looking,~~ scanning instrument modified from the nadir-looking airborne DIAL configuration first used in the 2006 Texas Air Quality Study (TexAQS II) (Alvarez et al., 2011; Senff et al., 2010). The lidar transmitter is based on a Ce:LiCAF laser pumped by a quadrupled Nd:YLF laser to produce three UV wavelengths, each at a 333 Hz repetition rate and tunable from 283 nm to 310 nm. The actual wavelengths used during DISCOVER-AQ 2014 were 287, 291, and 294 nm. Compared to the conventional two-wavelength DIAL, the three-wavelength configuration can potentially minimize the aerosol interference by using the dual-DIAL retrieval technique (Kovalev and Bristow, 1996) without assuming a lidar ratio and Angström exponent. However, in this study, ozone was retrieved using the 287- and 294-nm lidar signals and the standard two-wavelength DIAL algorithm because the two-wavelength retrieval was less affected by significant lidar signal noise (Alvarez et al., 2011).

Laser light backscattered by air molecules and aerosol particles is collected with a co-axial 50-cm diameter Newtonian telescope and then split at a 1:9 ratio into near- and far-field detection channels. The FOVs of the near- and far-field channels are controlled by different-size apertures resulting in full overlap at distances of ~300 m and ~800 m, respectively. Both channels use gated photomultipliers (PMTs) operated in analog mode with solar interference filters during the daytime. Compared to photon counting (PC) signals, the analog signal is able to ~~keep~~ maintain high linearity for strong signals and is particularly suitable for near-range measurements. The two-axis scanner on the truck sequentially ~~permits pointing~~points the laser beam at ~~several shallow elevation angles at a fixed, but changeable azimuth angle, typically at~~ 2°~~º~~, 6°~~º~~, 20°~~º~~, and 90°~~º~~ elevation angles in a cycle taking~~that are repeated~~ approximately ~~every~~ 5 minutes. The azimuth angle was fixed throughout the experiment. The ozone profiles at these four angles are spliced together to create composite vertical profiles extending from 10 m to about 2 km AGL (Langford et al., 2016). The range resolution of the signal recording system is 6 m.

Formatted: Not Superscript/ Subscript

During the 2014 DISCOVER-AQ and FRAPPÉ campaigns, the TOPAZ ozone observations ~~at low elevation angles (2°, 6°, and 20°)~~ suffered from a slight, but consistent range-dependent bias created by an unknown source of noise in the data acquisition system. The cause of this noise remains unknown and attempts to correct the resulting bias were unsuccessful. This bias manifests itself primarily in the low elevation ~~-~~angle observations (2°, 6°, and 20°) because the signal levels and SNR are significantly lower compared to the measurements at 90°~~º~~. For these reasons, the low angle observations below 500 ~~-~~m were excluded from the comparisons reported within this study.

Formatted: Not Superscript/ Subscript

2.1.3 LMOL/NASA LaRC

The transmitter of LMOL consists of a diode-pumped Nd:YLF laser pumping a Ce:LiCAF tunable UV laser to obtain two wavelengths typically at 287.1 and 292.7 nm with a pulse energy of 0.2 mJ at 500 Hz for each wavelength. The lidar receiver system consists of a 40-cm telescope with a 1.4-mrad FOV to measure far field and another 30-cm telescope with an adjustable FOV to measure near field (De Young et al., 2017). The raw lidar signals are recorded with a 7.5-m range resolution. The LMOL data acquisition system operates in both analog and PC modes. In this study, LMOL measures ozone between 0.7 and 4.5 km. Ozone measurements for DISCOVER-AQ represent LMOL's very first remote deployment.

2.1.4 Lidar Data Processing and Retrieval Algorithms

The data processing and DIAL retrieval algorithms for the three TOLNet lidars are similar but not identical. Their details have been described by Alvarez et al. (2011), De Young et al. (2017), Langford et al. (2011), and Sullivan et al. (2015; 2014). Some basic procedures were applied on the raw lidar signals before retrievals, such as time integration (5 min for this study), dead-time correction (for PC only), background correction (subtraction), merging of PC and analog signals (for a system with both PC and analog channels), and signal-induced-bias (SIB) correction (Kuang et al., 2013). Some parameters are system dependent or empirical due to different equipment, such as the dead-time value, PC-analog timing offset, averaging range for background calculation, and SIB ~~simulation~~ function form. All groups agreed to use the Brion-Daumont-Malicet (BDM) ~~database~~ (Daumont et al., 1992; Malicet et al., 1995; Brion et al., 1993) ~~to calculate differential~~ ozone absorption cross-sections, which are temperature-dependent.

The ozone number density profile results from computing the derivative of the logarithm of the on-line to off-line signal ratios. Spatial (range) smoothing is usually necessary to improve the SNR and reduce the statistical errors. Various smoothing methods and their impacts on final lidar retrieval have been described by Godin et al. (1999). Both TROPOZ and LMOL groups applied a Savitzky-Golay (SG) filter with a 2nd degree polynomial on the derivative of the logarithm of the on-line to off-line signal ratios with an increasing window width to accommodate the quickly decreasing SNR. However, the SG window sizes for TROPOZ and LMOL are different due to different SNRs at each altitude. The TOPAZ group averaged lidar signal over 90 m and, then, smoothed the derivative of the logarithm of the signal ratios with a five-point least-square fit~~ting~~ in a 450-m ~~interval~~window. The different retrieval methodologies and parameters affect the effective vertical resolution of the retrieved ozone profiles [Leblanc et al., 2016a], as listed in Table 1. This effective resolution determines the capability of the lidars to resolve vertical ozone structure and is not equal to, but is associated with, the fitting window width.

All groups applied similar schemes to correct the aerosol interference. These schemes iteratively substitute derived ozone from the DIAL equation into the lidar equation to solve aerosol extinction and backscatter until both aerosol and ozone converge (Alvarez et al., 2011; Kuang et al., 2011; Sullivan et al., 2014). The differential aerosol backscatter and extinction were calculated with the approximation from Browell et al. (1985). Lidars directly measure the ozone number density, and all three groups used the same temperature and pressure profiles from co-located ozonesonde measurements for Rayleigh correction, ozone mixing-ratio calculations, and computation of the temperature dependent ozone absorption cross sections.

Merging between different altitude channels, either different telescopes or different optical channels of the same telescope, is challenging with limited methodologies reported in the literature (Kuang et al., 2011). It is difficult to specify a method for all groups because merging is system-dependent and is affected by many factors previously described. Therefore, the three lidar groups merge the ozone profiles at different altitudes optimized for their system and SNR levels such as the example method described by Sullivan et al. (2015). As a result, additional differences between systems can occur due to the ~~non-standardized~~ altitude channel merging.

2.1.5 Error budget of the lidar measurements

Only a brief description of the error budget of the lidar measurements is provided in this paper since the details have been discussed in the respective instrument papers (Alvarez et al., 2011; De Young et al., 2017; Sullivan et al., 2014). Table 2 presents the estimated daytime measurement uncertainties for 5 and~~or~~ 30-min integration time for the three lidars. Statistical ~~errors~~ uncertainties (Papayannis et al., 1990) arising from signal ~~and background noise~~ fluctuations are random errors and may be improved by additional averaging or smoothing. The ~~maximum~~ statistical uncertainty, often referred to as measurement precision, generally increases with range due to decreasing SNR and is different ~~ies~~ for the three lidars ~~are similar (20% for 5 min and 8% for 30 min) within~~ due to their different laser power, telescope sizes, and measurement~~able~~ ranges. ~~although they are different at the same altitude.~~ The uncertainty associated with background correction also increases with range because of decreasing signal levels. The uncertainty due to the saturation correction of the PC signals (Donovan et al., 1993) is also range dependent and typically maximizes at near range. The uncertainty arising from aerosol interference could be the largest systematic error source and can be minimized by using the appropriate correction algorithm (Eisele and Trickl, 2005; Immler, 2003; Sullivan et al., 2014). The absorption by sulfur dioxide (SO_2) varies significantly with wavelength in the Hartley band. For the TOPAZ and LMOL systems, the differential SO_2 absorption cross section (Rufus et al., 2003) is only about 1/8 of their differential ozone absorption cross section so that the SO_2 interference is negligible unless very high ambient SO_2 concentrations are present. For TROPOZ with the 289-299-nm pair, the differential absorption cross section of SO_2 is about half of the ozone differential absorption cross section resulting in 1-ppb SO_2 being registered as 0.5-ppb ozone. Under typical atmospheric condition when SO_2 concentrations are less than 2 ppb (Heikes et al., 1987) and ozone concentrations are about 60 ppb, the SO_2-induced error is less than 2% (Sullivan et al., 2014). However, SO_2 can cause a more significant ozone bias when high SO_2 concentrations are present such as in power plant or volcanic plumes. The estimated total lidar measurement uncertainties [Leblanc et

Formatted: Font: (Default) Times New Roman, 10 pt
Formatted: Font: (Default) Times New Roman, 10 pt
Formatted: Font: (Default) Times New Roman, 10 pt
Formatted: Subscript
Formatted: Subscript
Formatted: Subscript
Formatted: Font: (Default) Times New Roman, 10 pt
Formatted: Font: (Default) Times New Roman, 10 pt
Formatted: Font: (Default) Times New Roman, 10 pt
Formatted: Subscript
Formatted: Font: (Default) Times New Roman, 10 pt
Formatted: Font: (Default) Times New Roman, 10 pt
Formatted: Subscript
Formatted: Font: (Default) Times New Roman, 10 pt
Formatted: Font: (Default) Times New Roman, 10 pt
Formatted: Font: (Default) Times New Roman, 10 pt, Subscript
Formatted: Font: (Default) Times New Roman, 10 pt
Formatted: Font: (Default) Times New Roman, 10 pt
Formatted: Font: (Default) Times New Roman, 10 pt
Formatted: Font: (Default) Times New Roman, 10 pt
Formatted: Font: (Default) Times New Roman, 10 pt
Formatted: Font: (Default) Times New Roman, 10 pt, Subscript
Formatted: Font: (Default) Times New Roman, 10 pt
Formatted: Font: (Default) Times New Roman, 10 pt, Subscript
Formatted: Font: (Default) Times New Roman, 10 pt
Formatted ...
Formatted ...
Formatted ...
Formatted ...
Formatted ...

al., 2016b] for a 30-min signal integration time are less than 20~~2~~%, 12%, and 13% for ~~5 and 30 min,~~TROPOZ, TOPAZ, and LMOL, respectively, within the lidar measurement ranges listed in Table 1.

2.2 Ozonesondes

An ozonesonde is a lightweight, balloon-borne instrument that consists of an ~~Teflon~~ air pump and an ozone sensor interfaced to a meteorological radiosonde. Ozonesondes are capable of measuring ozone under various weather conditions (e.g., cloudy, thunderstorm). The ozone sensor uses an ~~electrode~~ electrochemical concentration cell (ECC) containing potassium iodide (KI) solution (Komhyr, 1969; Komhyr et al., 1995) to measure ozone with a precision better than ±5% and an accuracy better than ±10% up to 35 km altitude with a sampling interval of about 1 s and a retrieval vertical resolution of 100 m (Deshler et al., 2008; Johnson et al., 2008; Smit et al., 2007). A radiosonde attached in the same package measures air temperature, pressure, and relative humidity (Stauffer et al., 2014). The uncertainty of ozonesonde measurements ~~is~~ is typically larger in the troposphere than that in the stratosphere (Liu et al., 2009). It has been reported that the ECC sondes suffer interference from SO_2 (Flentje et al., 2010) with 1-ppb SO_2 being registered as -1-ppb ozone (Schenkel and Broder, 1982). Elevated SO_2 can be a concern for lidar-ozonesonde intercomparison for some lidar wavelengths (e.g., 289-299 nm) because of the opposite signs of the measurement error arising from SO_2 for lidar and ozonesondes. However, this is not an issue for this study since we did not find any noticeable interference from SO_2 in either lidar or ozonesonde data. ~~As the balloon carrying the instrument package ascends through the atmosphere, the pump bubbles ambient air into the sensor cell. The reaction of ozone and iodide generates an electrical signal proportional to the amount of ozone. A radiosonde attached in the same package measures air temperature, pressure, and relative humidity (Stauffer et al., 2014). Ozonesondes are capable of measuring ozone under various weather conditions (e.g., cloudy, thunderstorm). The free-flying ozonesondes typically reach 35 km altitude in less than two hours with a rise rate at about 5 m/s.~~

Formatted: Subscript

Formatted: Subscript

Formatted: Subscript

2.3 Ozone Measurement Instrument onboard NASA's P-3B

NASA's P-3B aircraft is a pressurized, four-engine turboprop, capable of long-duration flights of 8-12 hours and is based out of NASA's Wallops Flight Facility in Wallops Island, Virginia. A series of gas and aerosol instruments were outfitted within the P-3B aircraft. Ozone was measured using the National Center for Atmospheric Research (NCAR)'s 4-channel chemiluminescence instrument based on the reaction between ambient ozone and nitric oxide (NO) with an accuracy of about ±5% and sampling interval of 1 s (Weinheimer et al., 1993; Ridley et al., 1992). The precision of this ozone detector is better than ±1% when ambient ozone is higher than 10 ppbv. The P-3B aircraft flew spirals from 300 m to 4570 m above the surface over selected ground monitoring sites including all three lidar sites (more information in Section 3.3) during the DISCOVER-AQ 2014 campaign.

3. Results

3.1 Lidar Intercomparisons

The three TOLNet lidars were deployed next to the BAO tower to take simultaneous measurements before the DISCOVER-AQ/FRAPPÉ campaign. They were only a few hundreds of meters away from each other and were within 5 m of the same elevation (see measurement locations in Table 1).

Unlike stratospheric ozone lidars that focus on integrating hours of observations (Steinbrecht et al., 2009; McDermid et al., 1990), tropospheric ozone lidars need to detect ozone variations with timescales on the order of minutes, when considering ozone's shorter lifetime, smaller-scale transport, and mixing processes within the PBL and free troposphere~~(Steinbrecht et al., 2009; McDermid et al., 1990)~~. Therefore, we processed all lidar data on a 5-min temporal scale (signal integration time). Rayleigh correction was performed with the same atmospheric profile from the ozonesonde. Because the three lidars have different fundamental range resolutions, retrieved ozone number density values were internally interpolated on the same altitude grid with a 15-m interval for comparison.

Field Code Changed

Field Code Changed

Figure 1 presents the comparison of the TOPAZ and TROPOZ observed ozone at BAO from 1300 to 2135 UTC (~~6 hours ahead of~~ local ~~time~~, Mountain Daylight Time, is UTC-6) on July 11, 2014 under a partly cloudy sky condition. Data influenced by clouds ~~interferences~~ were filtered out. Ozone time-height curtains from both lidars (Figure 1 a and b) show a significant (about 40%) ozone increase in the early afternoon. A total of 7655 TOPAZ and TROPOZ coincident pairs were constructed between 0.6 and 2 km AGL (altitude range over which both lidars provided valid data) over this time period. The measurement differences between the two lidars are mostly within ±5% at individual grids (Figure 1 c). The ~~product~~ value of averaged ozone concentration over some specified altitude range can represent the atmospheric ozone abundance and can be ~~also~~ useful for satellite validation. Here, we refer to this value ~~product~~ as ozone column average with the unit of number density, not to be confused with integrated column ozone often reported in Dobson units. The statistics of the intercomparison of the column averages is listed in Table 3. The similar 1σ standard deviations (17.8 and 16.7 x 10^{16} molec·m^{-3}) suggest similar ozone variations captured by both lidars (also see Figure 1 a and b). The mean relative difference (or normalized bias) was calculated by averaging the relative difference (i.e., (TROPOZ-TOPAZ)/TOPAZ, the denominator was arbitrarily chosen) for all paired ozone profiles. The -1.1±2.6% mean relative difference suggests excellent agreement of the averaged ozone column (Figure 1 d) for 80 profiles over 6.5 hours between TOPAZ and TROPOZ retrievals.

Figure 2 shows the TOPAZ-LMOL intercomparison for data taken on July 16, 2014 with 1902 coincident pairs from 0.9 to 2 km and between 1340 to 1730 UTC on this day. Some of the data gaps were due to low clouds blocking the lidar beams. The retrievals between the two lidars agree with each other mostly within ±10% (Figure 2 c). LMOL measured a mean ozone column average (Figure 2 d) 3.8±2.9% lower than TOPAZ for a total of 28 paired profiles, which is significantly fewer than those from the TROPOZ-TOPAZ comparison. This small, but statistically significant ozone column difference could be due to errors in the background and saturation corrections, or biases introduced by the merging of signals or ozone retrievals from different instrument channels. Almost the same 1σ of ozone column average in Table 3 suggests that the two lidars measured similar temporal ozone variations. The 1-σ bars on the column average in Figure 2 (d) represent the vertical ozone variability captured by lidar at a certain time. It can be seen that the two lidars measured highly similar vertical variability as well. The consistency in capture of ozone variability for TOPA and LMOL is in part due to their similar statistical uncertainties and vertical resolutions.

The generally random distribution of the relative differences in Figure 1 (c) and 2 (c) suggests overall consistent measurements with small systematic errors from all three lidars. In summary, TROPOZ, LMOL, and TOPAZ report ozone values at individual altitudes mostly within ±10%, which is well within their respective uncertainties and report ozone column averages within ±3.8% on average.

3.2 Lidars versus Ozonesondes

In order to compare the lidar data to ozonesondes, the Rayleigh- and aerosol-corrected lidar data was converted from ozone number densities to ozone mixing ratios by using sonde-measured pressure and temperature profiles, and averaged over a 30-minute interval (±15 minutes around sonde launch times). ~~.~~ Ozonesondes and lidars do not sample exactly the same atmospheric volume because the sondes typically drift horizontally. Therefore, discrepancies between the lidar and sonde observations may be in part due to real atmospheric differences. The horizontal displacement of the sonde usually increases with altitude, so the distance between sonde and lidar is normally larger in the free troposphere than in the PBL. However, horizontal ozone gradients tend to be smaller in the free troposphere than in the PBL, which typically keeps atmospheric differences rather small despite the increased displacement of the sonde. The ozonesondes report values approximately every second (about every 5 m in altitude) in raw data. For comparison, the ozonesonde raw data were linearly interpolated on the lidar altitude grids with a 15-meter interval. Figure 3 shows the mean ozone mixing ratios measured by TOLNet lidars and ozonesondes, as well as their mean relative difference as function of altitude.

After the DISCOVER-AQ/FRAPPÉ campaign started, the TROPOZ lidar deployed to Fort Collins, CO to measure ozone. There were 11 ozonesonde profiles that were coincident and co-located with the TROPOZ measurements. The mean ozone profiles of TROPOZ and sondes (Figure 3a) show similar vertical variations with enhanced PBL and upper tropospheric ozone. The mean relative differences between TROPOZ and ozonesondes (black line in Figure 3b) are mostly within ±10% up to 9 km. The local maximum of the differences at 1.8 km is associated with the merging of ozone retrievals from the near-field channel and far-field channel. The green lines in Figure 3 (b) represent the expected total measurement uncertainties including the lidar measurement uncertainties for a 30-min integration time (also see Table 2) and a 10% constant uncertainty for ozonesondes. The purple lines represent the 1-σ standard deviations of the mean differences, which can be compared to the combined precision of lidar (i.e., statistical uncertainty) and ozonesonde (5%). The 1-σ standard deviation increases from about 10% in the lower troposphere to about 20% in the upper troposphere as a result of increasing lidar statistical uncertainties with altitude. Below 9 km, the 1-σ standard deviations of the mean differences are mostly located within the range of the expected uncertainties. In particular, the lidar-sonde differences around 0.5 km are significantly less than the expected uncertainties suggesting that the detection and counting systems of TROPOZ performed better than anticipated. Above 9 km, the biases ~~start to~~ increase and exceed 25% with large oscillations due to large statistical errors as a consequence of low SNR. However, ozone observations with ~~B~~biases between 10-20% are still ~~very~~ representative of the upper free troposphere. On average, ~~for altitudes from 0.35 to 12 km,~~ TROPOZ measures 2.9% higher ozone than the ozonesondes for altitudes from 0.35 to 12 km. This difference can be seen as the mean difference of ozone column average between the ozonesondes and lidar for a 30-min integration time.

Formatted: Font: 10 pt, Not Bold
Formatted: Font: 10 pt
Formatted: Font: 10 pt, Not Bold
Formatted: Font: 10 pt
Formatted: Font: 10 pt, Not Bold
Formatted: Font: 10 pt
Formatted: Font: 10 pt, Not Bold
Formatted: Font: 10 pt, Not Bold
Formatted: Font: 10 pt
Formatted: Font: 10 pt, Not Bold

Between July 10 and July 16, a total of 10 ozonesondes were released near the BAO tower and 7 of them were coincident with TOPAZ measurements (3 on July 10, 3 on July 11, and 1 on July 16). TOPAZ mostly agrees with ozonesondes between -5% and 10% (black line in Figure 3 ~~c,~~ d). The 1-σ standard deviation of the mean differences (purple lines) is about 5% which is close to the combined precision of TOPAZ and ozonesondes (about 6%). 1-σ of the mean differences stays almost entirely within the expected uncertainties indicative of a proper estimate of the lidar measurement uncertainties for TOPAZ in Table 2. Compared to ozonesondes, TOPAZ measures 4.4% more PBL ozone on average**.**

On July 16, there was only one pair of coincident LMOL and ozonesonde measurements at the BAO tower (Figure 3 e, f). The 30-minute averaged LMOL ozone profile agrees with the ozonesonde mostly within 0-15% between 0.95 and 4.5 km AGL with an overall average of 6.2%**.** The maximum bias occurring at far range (above 4 km) is principally due to low SNR. The bias observed at 1.5 km is likely due to the high variation in aerosol concentration and associated uncertainties in the aerosol correction.~~, that was also observed in the green channel.~~ Since there is only one LMOL-ozonesonde comparison~~ between the LMOL and ozonesonde~~, the statistical information on the overall bias between their measurements is not available.

In summary, all three TOLNet lidars ~~exhibit overall positive bias~~measured higher ozone ~~, up to 4.4%,~~ ~~compared to~~than ozonesondes with mean ozone column differences of 2.9 % for TROPOZ, 4.4% for TOPAZ, and 6.2 % for LMOL (based on a single profile comparison). ~~excluding the single profile comparison to LMOL (6.2%)~~. ~~The larger bias than the~~ The differences between the two types of instruments and the standard deviations are mostly less than the expected uncertainties. ~~climatological difference between lidar and ozonesondes reported by Gaudel et al. (2015) (0.6 ppbv) could be associated with the much shorter averaging time period.~~ The ~~maximum~~ largest biase~~s~~ ~~exist~~ occurs at ~~in two regions, near range altitudes and~~ far-range altitudes~~. The large far range bias is~~ as expected and ~~is~~ is primarily associated with the high statistical errors arising from low SNR. The ~~large~~ increased bias at near-range ~~bias~~ altitudes ~~is more complicated and~~ could be associated with various factors, primarily the aerosol correction and the merging of the signals or ozone retrievals from different optical or altitude channels.

Formatted: Justified

3.3 Lidars versus P-3B Chemiluminescence Instrument

During the campaigns, the P-3B aircraft measured ozone profiles while doing spirals above the lidar sites. There are 34 coincident profiles between TROPOZ and the P-3B at Fort Collins, 29 between TOPAZ and the P-3B at the BAO tower, and 9 between LMOL and the P-3B at Golden, CO. The distances between the lidar and the P-3B spiral centers for these paired profiles were less than 11 km. To make coincident pairs between P-3B and lidar data, we interpolate the P-3B data onto the lidar vertical grids with a 15-m vertical resolution. Figure 4 shows the average ozone profiles measured by the lidars and the P-3B as well as their mean relative differences. TROPOZ and the P-3B agree with each other within ±5% between 0.5 to 3.5 km (black lines in Figure 4~~ a~~, b) with a -0.8% overall average relative difference. The 1-σ standard deviation of the mean differences (purple lines in Figure 4 b) stays almost entirely within the expected uncertainties (green lines) which include both calculated lidar measurement uncertainties and a 5% constant uncertainty for the P-3B. TOPAZ agrees with the P-3B within -11% and 3% between 0.5 and 2 km (Figure 4 c, d) with a -2.7% overall average relative difference. TOPAZ underestimates the lower-PBL (<1.5 km) ozone compared to P-3B, but when compared to ozonesondes TOPAZ overestimates ozone at many of these same altitudes (see Figure 3 d). LMOL agrees with P-3B mostly within -5% and 0% above 1800 m and within -15% and -5% between 0.7-1.8 km (Figure 4 e, f) with a -4.9% overall average relative difference. The 1-σ standard deviation of the LMOL-P3-B relative differences is mostly between 5% and 8% and is close to their combined precision (6%). The 1-σ of the mean differences for both TOPAZ and LMOL (purple lines in Figure 4 d, f) stays within the expected uncertainty (green lines) except for the bottom altitudes.

In summary, TOPAZ and LMOL exhibited noticeable negative bias in the PBL compared to the P-3B while TROPOZ measured slightly lower than the P-3B. The differences between the ~~two~~ three lidars and the P-3B are not significantly correlated suggesting that these biases ~~problem was not~~were not caused by ~~likely from~~ the P-3B ozone instrument. These differences could at least in part be caused by the lidar systematic errors mentioned in Section 2.1.5, but could also reflect horizontal ozone variability across the P-3B spirals, which were up to 22 km in diameter~~.~~

4. Summary and Conclusions

Intercomparisons have been made between three of the six TOLNet ozone lidars (NASA GSFC's TROPOZ, NOAA ESRL's TOPAZ, and NASA LaRC's LMOL) and between the lidars and other *in situ* ozone measurement instruments using coincident data during the 2014 DISCOVER-AQ and FRAPPÉ campaigns at NOAA's BAO in Erie, CO. On average, TROPOZ, TOPAZ, and LMOL reported very similar ozone within their reported uncertainties for a 5-min signal integration time. The three lidars measured consistent ozone variations revealed in the lidar time-height curtains and in the distribution of their relative differences. From intercomparisons between the lidars and other instruments we find (1) All of the lidars measure higher ozone than ozonesondes with an average~~d~~ relative difference within 4.4%. The lidar profile measurements agree with the ozonesonde observations within -10-15% ~~in their measurable ranges~~ except at a few ~~near~~far-field altitudes. These results are generally consistent with Sullivan et al. (2015) from a similar ozonesonde-lidar intercomparison. (2) TROPOZ agrees with the P-3B chemiluminescence ~~I~~instrument below 3.5 km within ±5% with a small column-averaged relative difference of -0.8%. TOPAZ and LMOL exhibit a slightly larger bias mostly between -15% and 5% below 2 km compared to the P-3B with a column-averaged difference of -2.7% and -4.9%, respectively.

~~Overall, interc~~Comparisons ~~between themselves~~among the three TOLNet lidars and with *in situ* instruments suggest that the ~~TOLNet~~ lidars are capable of capturing high-temporal tropospheric-ozone variability and of measuring tropospheric ozone with an accuracy better than ±15% in terms of their vertical resolving capability and better than ±5% in terms of their column measurement. These lidars have sufficient accuracy for model evaluation and satellite validation (Liu et al., 2010). Since the 2014 campaigns, all of the TOLNET lidars have been modified to improve their stability and their accuracy. The validation of these upgraded lidars will be reported in a future paper.

Acknowledgement

Formatted: Font: Not Bold

Formatted: Font: Not Bold

This work is supported by the TOLNet program developed by the National Aeronautics and Space Administration (NASA)'s Science Mission Directorate and by the National Oceanic and Atmospheric Administration Earth System Research Laboratory. Dr. John T. Sullivan's research was supported by an appointment to the NASA Postdoctoral Program at the NASA Goddard Space Flight Center, administered by Universities Space Research Association under contract with NASA. The views, opinions, and findings contained in this report are those of the authors and should not be construed as an official NOAA, NASA, or U.S. Government position, policy, or decision.

Table 1. Specifications for the TOLNet lidars.

	TROPOZ	**TOPAZ**	**LMOL**
Transmitter			
Laser type	Nd:YAG pumped D_2, H_2 Raman cell	Nd:YLF pumped Ce:LiCAF	Nd:YLF pumped Ce:LiCAF
Wavelengths (nm)	288.9, 299.1	287, 291, 294	287.1, 292.7
Pulse Repetition Rate (Hz)	50	333	500
Pulse energy (mJ)	12 (299 nm), 16 (289 nm)	~0.06 for all wavelengths	0.2 for both wavelengths
Detection and data acquisition system			
Telescope diameter (cm)	45, 2.5	50	40, 30
FOV (mrad)	1 (45 cm), 10 (2.5 cm)	1.5 (far field channel), 3 (near field channel)	1.4 (far field channel), variable FOV (near field channel)
Signal detection type	PMT	PMT	PMT
Data acquisition type	PC	Analog	Analog and PC
Fundamental range resolution (m)	15	6	7.5
Instrument reference	(Sullivan et al., 2014)	(Alvarez et al., 2011)	(DeYoung et al., 2017)
DIAL retrieval			
DIAL retrieval and smoothing method	1^{st}-order (differential) SG filter with a 2^{nd} degree polynomial with an increasing window width applied on the derivative of the logarithm of the signal ratios	five-point least square fit~~ting~~ with a 450-m window applied on the derivative of the logarithm of the signal ratios	1^{st}-order (differential) SG filter with a 2^{nd} degree polynomial, with an increasing window width applied on the derivative of the logarithm of the signal ratios
Retrieval effective resolution (m)	~100 at 1 km degrading to ~800 at 10 km	~10 below 50 m, ~30 from 50 to 150 m, ~100 from 150 to 500 m, 315 above 500 m	225 below 3 km degrading to 506 above 3 km
Aerosol correction reference	(Kuang et al., 2011; Sullivan et al., 2014)	(Alvarez et al., 2011)	(Browell et al., 1985; DeYoung et al., 2017)
Valid altitudes (km above ground level, AGL)	0.35-16	0.01-2	0.7-4.5
Measurement location			
Latitude (^{o}N)	40.050	40.045	40.050
Longitude (^{o}W)	105.000	105.006	105.004
Elevation (m ASL)	1584	1587	1584

Table 2. ~~Estimated~~ Maximum 1-σ uncertainties for TROPOZ, TOPAZ and LMOL daytime ozone measurements within their measurable range ~~(see Table 1)~~ for the 5 and~~or~~ 30-min integration time.

Source	Maximum uncertainty within each lidar's measurement range					
	5-min integration			30-min integration		
Lidar	TROPOZ	TOPAZ	LMOL	TROPOZ	TOPAZ	LMOL
Measurement range (km)	0.35-16	0.01-2	0.7-4.5	0.35-16	0.01-2	0.7-4.5
Statistical Uncertainty[a]	20%	8%	15%	8%	3%	6%
Background correction[a]	10%	3%	5%	10%	3%	5%
Saturation correction[b]	1%	N/A	5%	1%	N/A	5%
Aerosol interference	10%	10%	10%	10%	10%	10%
Interference by SO_2, NO_2, O_2 dimer	3%	1%	1%	3%	1%	1%
Differential Rayleigh scattering	3%	3%	3%	3%	3%	3%
Ozone absorption cross section	3%	3%	3%	3%	3%	3%
Total uncertainty[c]	25%	14%	19%	20%	12%	13%

Formatted: Superscript

[a] Range dependent and increasing with altitude.

[b] Range dependent and typically maximized at the near range.

[c] Total root-mean-square uncertainty by considering the range dependent uncertainties (also see Figure 3 and 4).

~~*Total root-mean-square error.~~

Table 3. Comparisons of the ozone column average measured by TROPOZ, TOPAZ, and LMOL.

Date	UTC time range	Altitude range (km)	Lidar	Number of the paired profiles	Mean ozone column average (10^{16} molec·m^{-3})	1σ of the ozone column average (10^{16} molec·m^{-3})	Mean relative difference *	1σ of the difference
7/11/2014	1300 - 2135	0.6-2	TROPOZ/TOPAZ	80	127.3/128.6	17.8/16.7	-1.1%	2.6%
7/16/2014	1335 - 1730	0.9-2	LMOL/TOPAZ	28	98.1/102.0	13.1/13.0	-3.8%	2.9%

* Equal to mean (A-B)/B for A/B in 'Lidar' column for all paired profiles.

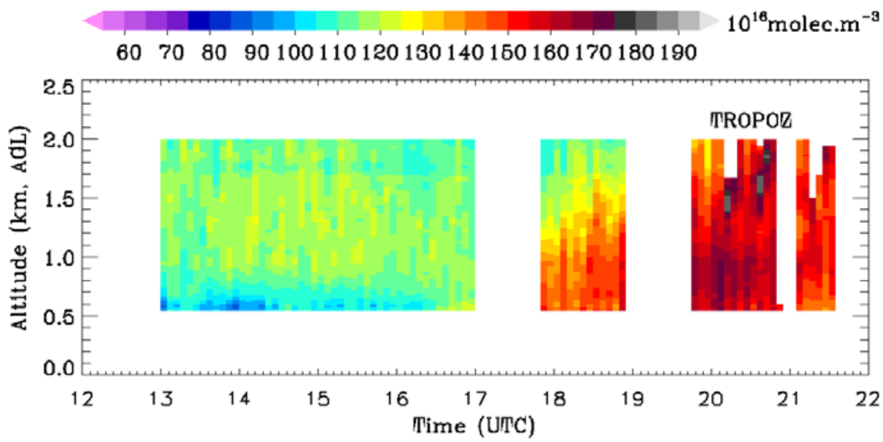
10^{16}molec.m^{-3}
60 70 80 90 100 110 120 130 140 150 160 170 180 190
TROPOZ
Altitude (km, AGL)
Time (UTC)

(a)

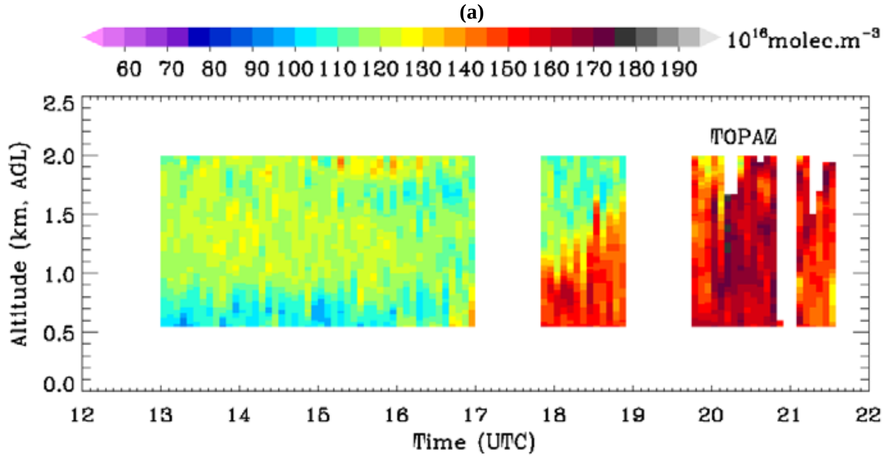
10^{16}molec.m^{-3}
60 70 80 90 100 110 120 130 140 150 160 170 180 190
TOPAZ
Altitude (km, AGL)
Time (UTC)

(b)

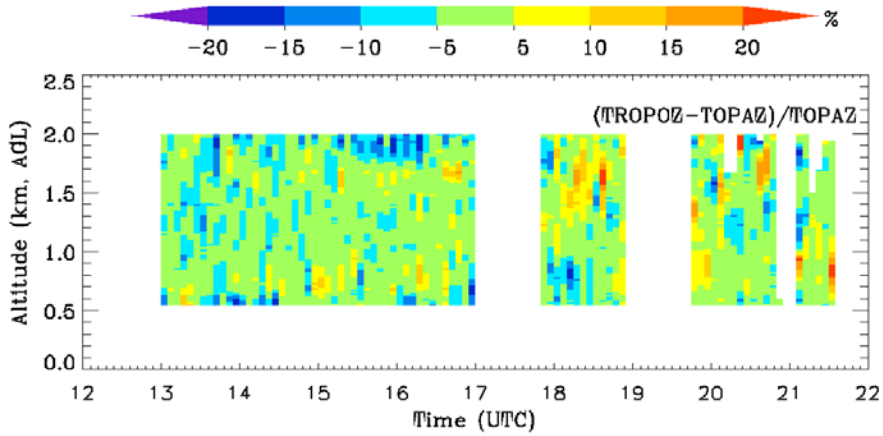

(c)

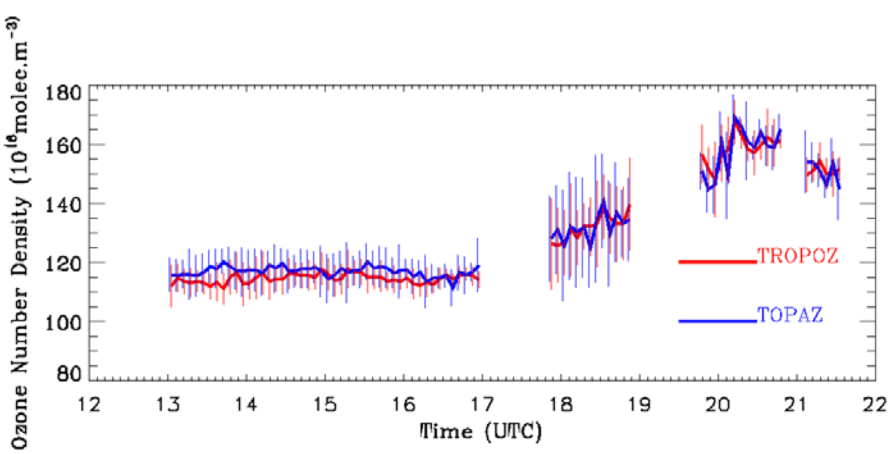

(d)

Figure 1. Comparisons of ozone measured by TROPOZ and TOPAZ. (a) Ozone number densities measured by TROPOZ. (b) Ozone number densities measured by TOPAZ. (c) Their relative percent differences, (TROPOZ-TOPAZ)/TOPAZ. (d) Column averages measured by the TROPOZ and TOPAZ as well as their 1-σ standard deviations. TROPOZ measures 1.1±2.6% lower ozone column average than TOPAZ.

Formatted: Font: (Default) Times New Roman, 10 pt

Formatted: Left, Indent: Left: 0"

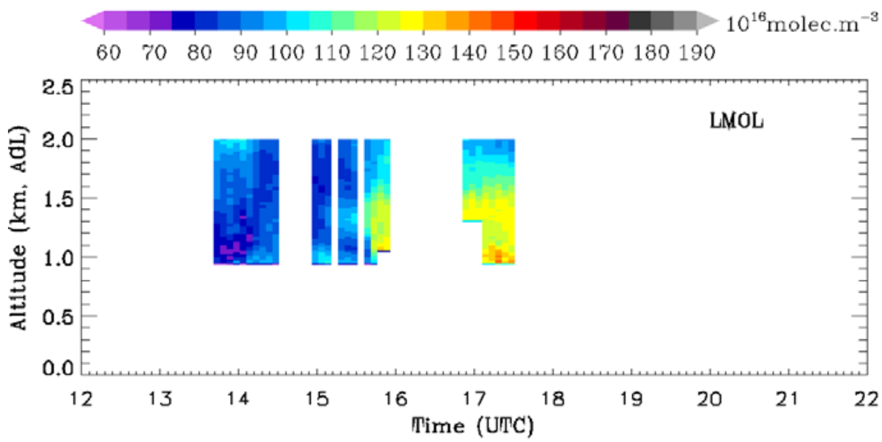

(a)

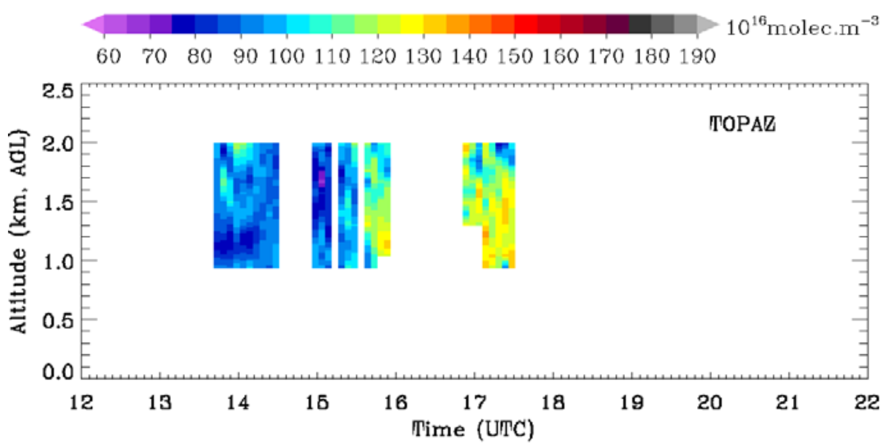

(b)

Formatted: Font: Not Bold

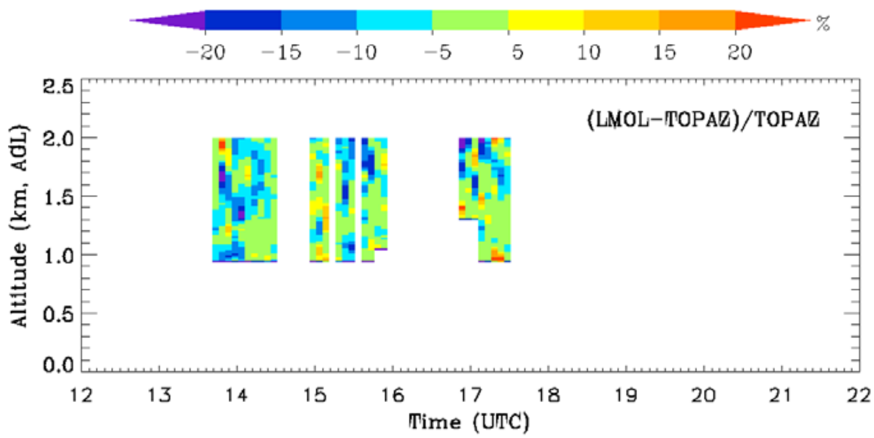

(c)

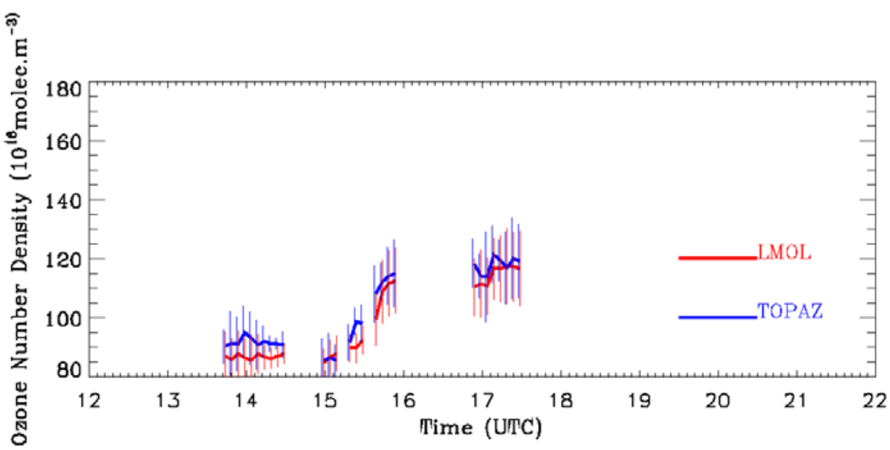

(d)

Figure 2. Comparisons of ozone measured by LMOL and TOPAZ. (a) LMOL-measured ozone number densities. (b) TOPAZ-measured ozone number densities. (c) Their relative percent differences, (LMOL-TOPAZ)/TOPAZ. (d) Column averages measured by LMOL and TOPAZ as well as their 1-σ standard deviations. LMOL measures 3.8±2.9% lower ozone column average than TOPAZ.

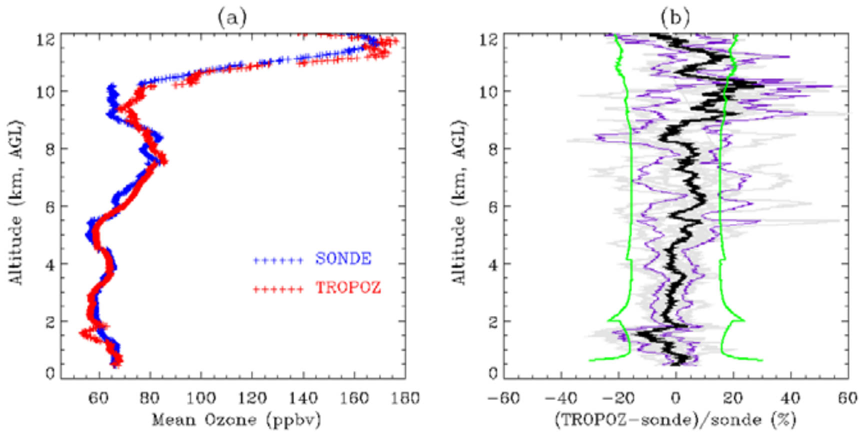
(a)
(b)
Altitude (km, AGL)
Mean Ozone (ppbv)
++++++ SONDE
++++++ TROPOZ
(TROPOZ−sonde)/sonde (%)

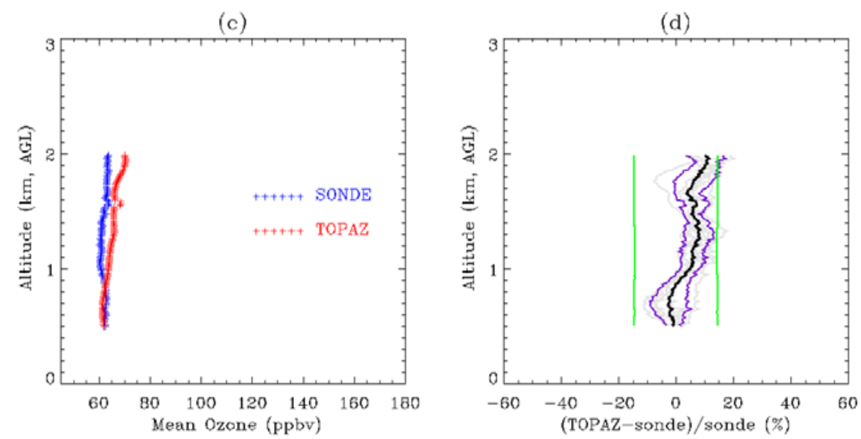
(c)
(d)
Altitude (km, AGL)
Mean Ozone (ppbv)
++++++ SONDE
++++++ TOPAZ
(TOPAZ−sonde)/sonde (%)

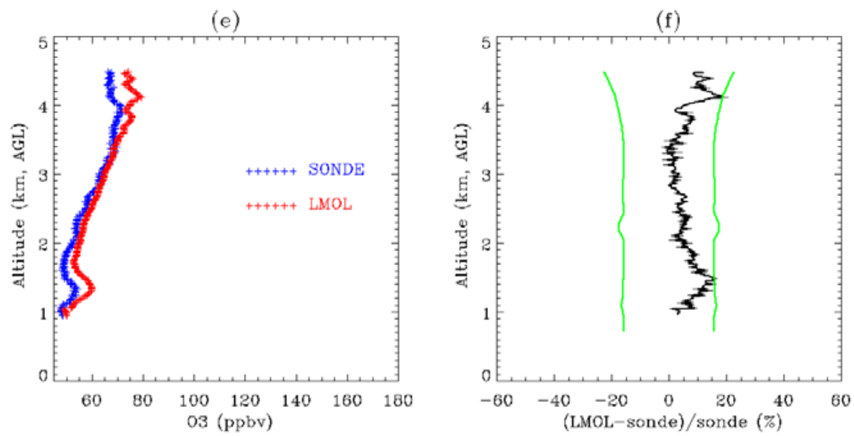

Figure 3. Comparisons of lidar and ozonesonde measurements. (a) Average ozone profiles measured by TROPOZ and ozonesondes at Fort Collins, CO (11 pairs). (b) Mean relative difference (black) between TROPOZ and ozonesondes as well as the 1-σ standard deviations (purple). (c) Average ozone profiles measured by TOPAZ and ozonesondes at BAO Tower (7 pairs). (d) Mean relative difference (black) between TOPAZ and ozonesondes as well as the 1-σ standard deviations (purple). (e) Average ozone profiles measured by LMOL and ozonesonde at the BAO tower (1 pair). (f) Relative difference between LMOL and ozonesonde. The gray lines represent the individual difference profiles between the lidar and sondes. The green lines represent the expected uncertainties including the 30-min lidar measurement uncertainties (also see Table 2) and a 10% constant uncertainty for ozonesondes.

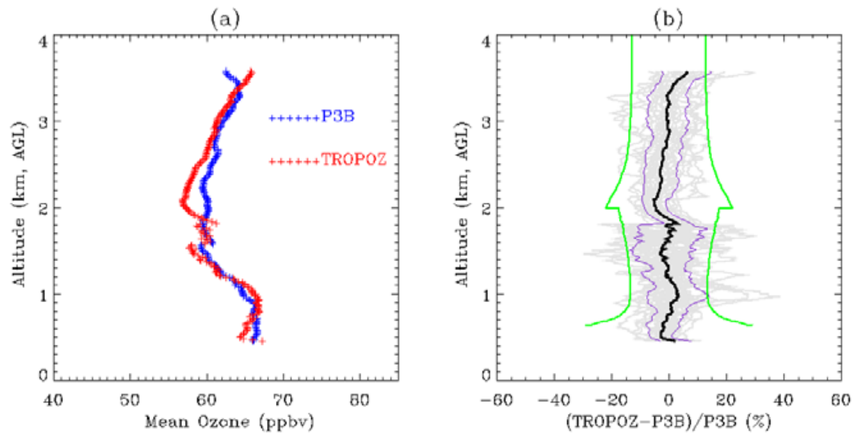
(a)
(b)
Altitude (km, AGL)
++++++P3B
++++++TROPOZ
Mean Ozone (ppbv)
(TROPOZ-P3B)/P3B (%)

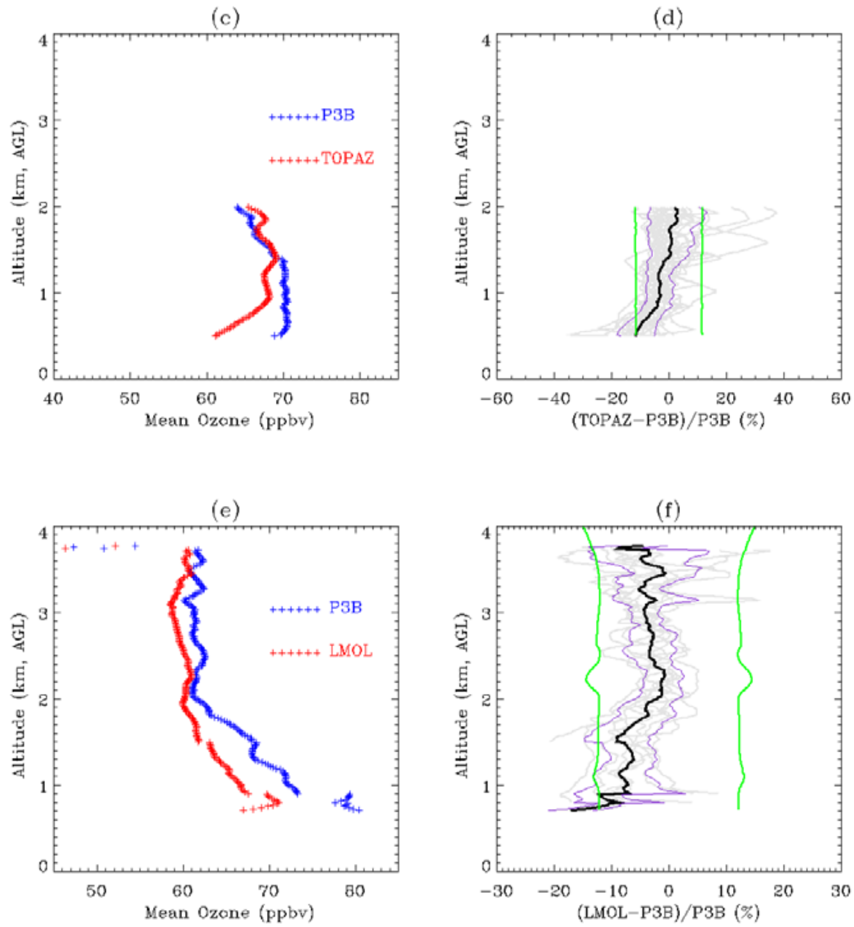

Figure 4. Intercomparison between the lidar and P-3B measurements. (a) Average ozone profiles measured by TROPOZ and P-3B at Fort Collins, CO (34 profiles). (b) Mean relative difference (black) between TROPOZ and P-3B data as well as the 1-σ standard deviation (purple). (c) Average ozone profiles measured by TOPAZ and P-3B at the BAO Tower (29 profiles). (d) Mean relative difference between TOPAZ and P-3B data as well as the 1-σ standard deviation (purple). (e) Average ozone profiles measured by LMOL and P-3B at Golden, CO (9 profiles). (f) Mean relative difference between LMOL and P-3B data as well as the 1-σ standard deviation (purple). The gray lines represent the individual difference profiles between the lidar and sondes. The green lines represent the expected uncertainties including the 30-min lidar measurement uncertainties (also see Table 2) and a 10% constant uncertainty for ozonesondes.

References

Alvarez, R. J., Senff, C. J., Langford, A. O., Weickmann, A. M., Law, D. C., Machol, J. L., Merritt, D. A., Marchbanks, R. D., Sandberg, S. P., Brewer, W. A., Hardesty, R. M., and Banta, R. M.: Development and Application of a Compact, Tunable, Solid-State Airborne Ozone Lidar System for Boundary Layer Profiling, J. Atmos. Oceanic Tech., 28, 1258-1272, 10.1175/JTECH-D-10-05044.1, 2011.

Bowman, K. W.: Toward the next generation of air quality monitoring: Ozone. Atmos. Environ., 80, 571-583, 2013.

Brion, J., Chakir, A., Daumont, D., and Malicet, J.: High-resolution laboratory absorption cross section of O3 temperature effect, Chem. Phys. Lett., 213, 510-512, 1993.

Browell, E. V., Ismail, S., and Shipley, S. T.: Ultraviolet DIAL measurements of O_3 profiles in regions of spatially inhomogeneous aerosols, Appl. Opt., 24, 2827-2836, 1985.

Crawford, J. H., and Pickering, K. E.: DISCOVER-AQ: Advancing strategies for air quality observations in the next decade, Environ. Manage, 4-7, 2014.

Daumont, D., Brion, J., Charbonnier, J., and Malicet, J.: Ozone UV spectroscopy I: Absorption cross-sections at room temperature, J. Atmos. Chem., 15, 145-155, 1992.

De Young, R., Carrion, W., Ganoe, R., Pliutau, D., Gronoff, G., Berkoff, T., and Kuang, S.: Langley mobile ozone lidar: ozone and aerosol atmospheric profiling for air quality research, Appl. Opt., 56, 721, 10.1364/ao.56.000721, 2017.

Deshler, T., Mercer, J. L., Smit, H. G. J., Stubi, R., Levrat, G., Johnson, B. J., Oltmans, S. J., Kivi, R., Thompson, A. M., Witte, J., Davies, J., Schmidlin, F. J., Brothers, G., and Sasaki, T.: Atmospheric comparison of electrochemical cell ozonesondes from different manufacturers, and with different cathode solution strengths: The balloon experiment on standards for ozonesondes., J. Geophys. Res., 113, D04307, doi: 10.1029/2007/JD008975, 2008.

Dingle, J. H., Vu, K., Bahreini, R., Apel, E. C., Campos, T. L., Flocke, F., Fried, A., Herndon, S., Hills, A. J., Hornbrook, R. S., Huey, G., Kaser, L., Montzka, D. D., Nowak, J. B., Reeves, M., Richter, D., Roscioli, J. R., Shertz, S., Stell, M., Tanner, D., Tyndall, G., Walega, J., Weibring, P., and Weinheimer, A.: Aerosol optical extinction during the Front Range Air Pollution and Photochemistry Éxperiment (FRAPPÉ) 2014 summertime field campaign, Colorado, USA, Atmos. Chem. Phys., 16, 207-217, doi:10.5194/acp-16-11207-2016, 2016.

Donovan, D. P., Whiteway, J. A. and Carswell, A. I.: Correction for nonlinear photon-counting effects in lidar systems, Appl. Opt., 32, 6742-6753, 1993.

Eisele, H., and Trickl, T.: Improvements of aerosol algorithm in ozone lidar data processing by use of evolutionary strategies, Appl. Opt., 44, 2638-2651, 2005.

Flentje, H., Claude, H., Elste, T., Gilge, S., Köhler, U., Plass-Dülmer, C., Steinbrecht, W., Thomas, W., Werner, A. and Fricke, W.: The Eyjafjallajökull eruption in April 2010–detection of volcanic plume using in-situ measurements, ozone sondes and lidar-ceilometer profiles, Atmos. Chem. Phys. 10, 10085-10092, 2010.

~~Gaudel, A., Ancellet, G. and Godin-Beekmann, S.: Analysis of 20 years of tropospheric ozone vertical profiles by lidar and ECC at Observatoire de Haute Provence (OHP) at 44 N, 6.7 E, Atmos. Environ., 113, 78-89, 2015.~~

Godin, S. M., Carswell, A. I., Donovan, D. P., Claude, H., Steinbrecht, W., McDermid, I. S., McGee, T. J., Gross, M. R., Nakane, H., Swart, D. P. J., Bergwerff, H. B., Uchino, O., Gathen, P. v. d., and Neuber, R.: Ozone differential absorption lidar algorithm intercomparison, Appl. Opt., 38, 6225-6236, 1999.

Heikes, B.G., Kok, G.L., Walega, J.G. and Lazrus, A.L.: H2O2, O3 and SO2 measurements in the lower troposphere over the eastern United States during fall, J. Geophys. Res.: Atmospheres, 92, 915-931, 1987.

Immler, F.: A new algorithm for simultaneous ozone and aerosol retrieval from tropospheric DIAL measurements, Appl. Phys. B, 76, 593-596, 2003.

Johnson, B. J., Helmig, D., and Oltmans, S.: Evaluation of ozone measurements from a tethered balloon-sampling platform at South Pole Station in December 2003, Atmos. Environ., 42, 2780-2878, 10.1016/j.atmosenv.2007.03.043, 2008.

Komhyr, W. D.: Electrochemical cells for gas analysis, Ann. Geophys., 25, 203-210, 1969.

Komhyr, W. D., Barnes, R. A., Brothers, G. B., Lanthrop, J. A., and Opperman, D. P.: Electrochemical concentration cell ozonesonde performance evaluation during STOIC 1989, J. Geophys. Res., 100, 9231-9244, 1995.

Formatted: No underline

Formatted: Font: (Default) Times New Roman, 10 pt

Formatted: Indent: Left: 0", Hanging: 0.5"

Kovalev, V. A., and Bristow, M. P.: Compensational three-wavelength differential-absorption lidar technique for reducing the influence of differential scattering on ozone-concentration measurements, Appl. Opt., 35, 4790-4797, 1996.

Kuang, S., Burris, J. F., Newchurch, M. J., Johnson, S., and Long, S.: Differential Absorption Lidar to Measure Subhourly Variation of Tropospheric Ozone Profiles, IEEE Transactions on Geoscience and Remote Sensing, 49, 557-571, 10.1109/TGRS.2010.2054834, 2011.

Kuang, S., Newchurch, M. J., Burris, J., and Liu, X.: Ground-based lidar for atmospheric boundary layer ozone measurements, Appl. Opt., 52, 3557-3566, 10.1364/AO.52.003557, 2013.

Langford, A. O., Senff, C. J., Alvarez II, R. J., banta, R. M., Hardesty, M., Parrish, D. D., and Ryerson, T. B.: Comparison between the TOPAZ airborne ozone lidar and in situ measurements during TexAQS 2006, J. Atmos. Oceanic Technol., 28, 1243-1257, doi: http://dx.doi.org/10.1175/JTECH-D-10-05043.1 2011.

Langford, A. O., Alvarez, R. J., Brioude, J., Fine, R., Gustin, M., Lin, M. Y., Marchbanks, R. D., Pierce, R. B., Sandberg, S. P., Senff, C. J., Weickmann, A. M., and Williams, E. J.: Entrainment of stratospheric air and Asian pollution by the convective boundary layer in the Southwestern U.S, Journal of Geophysical Research: Atmospheres, n/a-n/a, 10.1002/2016JD025987, 2016.

Leblanc, T., Sica, R. J., van Gijsel, J. A. E., Godin-Beekmann, S., Haefele, A., Trickl, T., Payen, G., and Gabarrot, F.: Proposed standardized definitions for vertical resolution and uncertainty in the NDACC lidar ozone and temperature algorithms – Part 1: Vertical resolution, Atmos. Meas. Tech., 9, 4029-4049, 10.5194/amt-9-4029-2016, 2016a.

Leblanc, T., Sica, R.J., Van Gijsel, J.A., Godin-Beekmann, S., Haefele, A., Trickl, T., Payen, G. and Liberti, G., 2016. Proposed standardized definitions for vertical resolution and uncertainty in the NDACC lidar ozone and temperature algorithms–Part 2: Ozone DIAL uncertainty budget. Atmospheric Measurement Techniques, 9(8), pp.4051-4078, 2016b.

Liu, G., Tarasick, D. W., Fioletov, V. E., Sioris, C. E. and Rochon, Y. J.: Ozone correlation lengths and measurement uncertainties from analysis of historical ozonesonde data in North America and Europe. J. of Geophys. Res., 114, D04112, 2009.

Liu, X., Bhartia, P. K., Chance, K., Spurr, R. J. D., and Kurosu, T. P.: Ozone profile retrievals from the Ozone Monitoring Instrument, Atmos. Chem. Phys., 10, 2521-2537, 2010.

Malicet, C., Daumont, D., Charbonnier, J., Parisse, C., Chakir, A., and Brion, J.: Ozone UV spectroscopy. II. Absorption cross-sections and temperature dependence, J. Atmos. Chem., 21, 263-273, 1995.

McDermid, I. S., Godin, S. M., Lindqvist, L. O., Walsh, T. D., Burris, J., Butler, J., Ferrare, R., Whiteman, D., and McGee, T. J.: Measurement intercomparison of the JPL and GSFC stratospheric ozone lidar systems, Appl. Opt., 29, 4671-4676, 1990.

Newchurch, M. J., Kuang, S., Leblanc, T., Alvarez, R. J., Langford, A. O., Senff, C. J., Burris, J. F., McGee, T. J., Sullivan, J. T., DeYoung, R. J., and Al-Saadi, J.: TOLNET - A Tropospheric Ozone Lidar Profiling Network for Satellite Continuity and Process Studies, The 27th International Laser Radar Conference (ILRC 27), 2016,

Papayannis, A., Ancellet, G., Pelon, J., and Mégie, G.: Multiwavelength lidar for ozone measurements in the troposphere and the lower stratosphere, Appl. Opt., 29, 467-476, 1990.

Ridley, B. A., Grahek, F. E., and Walega, J. G.: A small high-sensitivity, medium-response ozone detector suitable for measurements from light aircraft, J. Atmos. Oceanic Tech., 9, 142-148, 1992.

Rufus, J., Stark, G., Smith, P.L., Pickering, J.C. and Thorne, A.P.: High - resolution photoabsorption cross section measurements of SO2, 2: 220 to 325 nm at 295 K, J. Geophy. Res.: Planets, 108, 2003

Schenkel, A., and Broder, B.: Interference of some trace gases with ozone measurements by the KI method, Atmos. Environ., 16, 2187-2190, 1982.

Senff, C. J., Alvarez, R. J., Hardesty, R. M., Banta, R. M., and Langford, A. O.: Airborne lidar measurements of ozone flux downwind of Houston and Dallas, J. Geophys. Res.: Atmospheres, 115, ~~n/a-n/a~~D20, 10.1029/2009JD013689, 2010.

Smit, H. G. J., Straeter, W., Johnson, B. J., Oltmans, S. J., Davies, J., Tarasick, D. W., Hoegger, B., Stubi, R., Schmidlin, F. J., Northam, T., Thompson, A. M., Witte, J. C., Boyd, I., and Posny, F.: Assessment of the performance of ECC-ozonesondes under quasi-flight conditions in the environmental simulation chamber: Insights from the Juelich Ozone Sonde Intercomparison Experiment (JOSIE), J. Geophys. Res., 112, D19306, doi:10.1029/2006JD007308, 2007.

Stauffer, R. M., Morris, G. A., Thompson, A. M., Joseph, E., Coetzee, G. J. and Nalli, N. R.: Propagation of radiosonde pressure sensor errors to ozonesonde measurements, Atmos. Meas. Tech., 7, 65-79, 2014.

Formatted: Font: (Default) Times New Roman, 10 pt

Formatted: Font: (Default) Times New Roman, 10 pt, No underline, Font color: Auto

Formatted: Font: (Default) Times New Roman, 10 pt, Not Italic

Formatted: Font: (Default) Times New Roman, 10 pt

Formatted: Font: (Default) Times New Roman, 10 pt, Not Italic

Formatted: Font: (Default) Times New Roman, 10 pt

Formatted: Font: (Default) Times New Roman, 10 pt

Formatted: Font: (Default) Times New Roman, 10 pt, No underline, Font color: Auto

Formatted: Font: (Default) Times New Roman, 10 pt

Formatted: Font: (Default) Cambria Math, 10 pt

Formatted: Font: (Default) Times New Roman, 10 pt

Formatted: Font: (Default) Times New Roman, 10 pt

Formatted: Font: (Default) Times New Roman, 10 pt, Not Italic

Formatted: Font: Not Italic

Formatted: Font: (Default) Times New Roman, 10 pt, Not Italic

Formatted: Font: Not Italic

Formatted: Font: (Default) Times New Roman, 10 pt, Not Italic

Formatted: Font: Not Italic

Formatted: Font: (Default) Times New Roman, 10 pt, Not Italic

Formatted: Font: (Default) Times New Roman, 10 pt

Formatted: Font: (Default) Times New Roman, 10 pt, Not Italic

Formatted: Font: 10 pt

Formatted: Font: (Default) Times New Roman, 10 pt

Formatted: Font: 10 pt

Formatted: Font: (Default) Times New Roman, 10 pt, Not Italic

Formatted: Font: (Default) Times New Roman, 10 pt

Formatted: Font: 10 pt

Formatted ...

Formatted: No underline

Steinbrecht, W., McGee, T. J., Twigg, L. W., Claude, H., Schönenborn, F., Sumnicht, G. K., and Silbert, D.: Intercomparison of stratospheric ozone and temperature profiles during the October 2005 Hohenpeißenberg Ozone Profiling Experiment (HOPE), Atmos. Meas. Tech., 2, 125-145, 2009.

Sullivan, J. T., McGee, T. J., Sumnicht, G. K., Twigg, L. W., and Hoff, R. M.: A mobile differential absorption lidar to measure sub-hourly fluctuation of tropospheric ozone profiles in the Baltimore-Washington, D.C. region, Atmos. Meas. Tech., 7, 3529-3548, 10.5194/amt-7-3529-2014, 2014.

Sullivan, J. T., McGee, T. J., DeYoung, R., Twigg, L. W., Sumnicht, G. K., Pliutau, D., Knepp, T., and Carrion, W.: Results from the NASA GSFC and LaRC Ozone Lidar Intercomparison: New Mobile Tools for Atmospheric Research, J. Atmos. Oceanic Tech., 32, 1779-1795, doi:10.1175/JTECH-D-14-00193.1, 2015.

Weinheimer, A. J., Walega, J. G., Ridley, B. A., Sache, G. W., Anderson, B. E., and Collins Jr., J. E.: Stratospheric NOy measurements on the NASA DC-8 during AASE II, Geophys. Res. Lett., 20, 2563-2566, 1993.